Hans 汉斯

布里奇曼石的晶体结构及物理性质

魏雪会

北京高压科学研究中心，北京
Email: xuehui.wei@hpstar.ac.cn

摘　要

布里奇曼石(bridgmanite)是地球上最丰富的矿物，能够稳定存在于下地幔的极端高温高压环境中。布里奇曼石的晶格中有一定量的Fe和Al，这导致它的晶体结构复杂。化学成分的变化会引起结构的改变，进而对其密度、压缩性、电导率等物理性质产生影响。布里奇曼石的物理性质是理解下地幔动力学、地幔对流、弹性性质等的关键，并且为地震波速异常可能提供解释。

关键词

布里奇曼石，晶体结构，Fe和Al的占位，X-Ray衍射

Crystal Structure of Bridgmanite and Its Physical Properties

Xuehui Wei

Center for High Pressure Science & Technology Advanced Research, Beijing
Email: xuehui.wei@hpstar.ac.cn

Abstract

Bridgmanite, remaining stable under extremely high temperature and pressure conditions of the earth's lower mantle, is the most abundant mineral on the earth. Doping with small doses of Fe and Al in its lattice, bridgmanite crystallography is fairly complex. Variation of chemical compositions causes changes in crystal structure, which in turn influences density, compressibility, electrical conductivity and other physical properties significantly. Physical property of bridgmanite is the key to understand lower mantle dynamics, mantle convection, elasticity, as well as anomalies of seismic velocities.

Keywords

Bridgmanite, Crystal Structure, Occupation of Fe and Al, X-Ray Diffraction

1. 引言

晶体结构是矿物的最基本的性质，并且与矿物的诸如压缩性、密度、声速等物理性质密切相关。比如，下地幔的底部的地震波各向异性与矿物的弹性各向异性有关，而各向异性最终是由矿物的化学成分和晶体结构导致的。晶体结构也能强烈影响不同相之间的元素分配以及下地幔的化学状态[1] [2] [3]。

对于下地幔的矿物相组成，地幔橄榄岩模型接受程度较广(图 1)。地幔橄榄岩是基于对地幔顶部橄榄岩和玄武岩的实验和岩石学研究，假设下地幔的成分与上地幔成分总体相似[4]。在地幔橄榄岩中，布里奇曼石、方镁石和钙硅钙钛矿是下地幔范围的矿物[5] [6]。地球物理学证据显示俯冲的大洋岩石圈能穿透660 km 的不连续面，因此，在地幔深处的大洋俯冲板块很可能到达了核幔边界。伴随着钙硅钙钛矿(Ca-perovskite)、自由硅和含铝相的增加，俯冲的玄武岩板块可能会产生不同的矿物组成[7]。
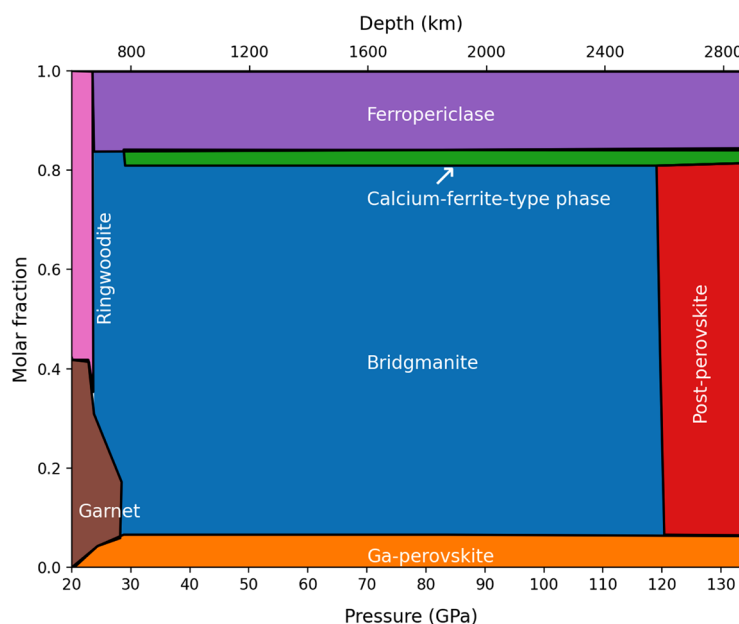

Figure 1. Modal fractions of mantle phases for the pyrolite compositional models
图 1. 下地幔地幔橄榄石的矿物相组成

2. 布里奇曼石的晶体结构

布里奇曼石$(Mg, Al) (Al, Si, Fe)O_3$是下地幔的主要矿物相，也是地球上最丰富的矿物[8]。实验测试和理论计算显示布里奇曼石大概占据下地幔体积的75%，而方镁石和钙钛矿各占体积的20%和5% [9] [10]，然而也有人预计布里奇曼石的体积比大概是93% [11]。尽管布里奇曼石在实验室中可以被淬火到室温条

件得到，直到2014年才在球粒陨石中发现天然样本[$(Mg_{0.75}Fe_{0.20}Na_{0.03}Ca_{0.02}Mn_{0.01})SiO_3$] [8]，并被命名为布里奇曼石(bridgmanite)。布里奇曼石的形成的压力和温度条件大概是23~25 GPa，2200~2400 K。

布里奇曼石的化学式为ABO_3，斜方晶系，空间群是 *Pbnm* [12]。在布里奇曼石的晶体结构中有两种阳离子位置，A位被大半径阳离子占据，B位容纳小半径阳离子。钙钛矿的结构可以被描述为SiO_6八面体形成的共顶点的框架结构，同时A填充结构中的框架(图2)。
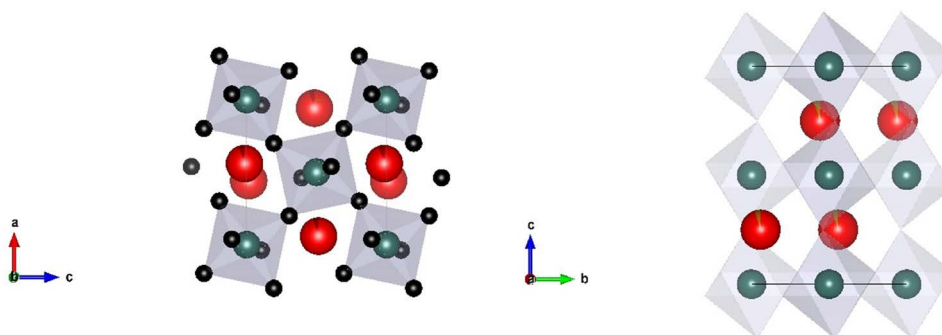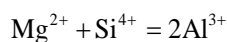

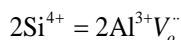**Figure 2.** View along the b (left) and a axis (right) of bridgmanite
图 2. 沿 b 轴和 a 轴观察布里奇曼石

钙钛矿的理想结构是立方型晶体(空间群是 $Pm\bar{3}m$)，通过八面体的旋转和扭曲，或者阳离子的替代和非化学计量，形成多种其他的结构类型[13]，如四方、正交和单斜等对称型。SiO_6通过八面体相对于 *c* 轴的旋转和扭曲以及中心 Mg 原子位置的偏移实现从理想的立方型到正交型的转变: $(a, b, c)_{Pnma} \rightarrow (b, c, a)_{Pbnm}$。随着压力升高，结构畸变增强[14]。

3. 布里奇曼石中的 Fe 和 Al

地幔橄榄岩模型含有~10 wt%的 Fe 和~5 wt%的 Al，理论计算和实验表明高压下，布里奇曼石本身能容纳更多的 Fe 和 Al [15]。前人的实验结果表明，Fe^{2+}取代 A 位的Mg^{2+}会使结构膨胀[16]。而Fe^{3+}可以取代Mg^{2+}和Si^{4+}，同样能够扩大结构，但是会增大畸变程度[17]。而 Al 进入布里奇曼石结构的方式有两种，即耦合化学计量取代:

$$Mg^{2+} + Si^{4+} = 2Al^{3+}$$

或者是通过非化学计量替代，即包含一个氧空位$V_o^{\cdot\cdot}$:

$$2Si^{4+} = 2Al^{3+}V_o^{\cdot\cdot}$$

在下地幔的压力条件下，能量上支持化学计量替代[3] [18] [19]，但是也有实验表明，两种替代方式可以在实验室合成的布里奇曼石样本中共存。核磁共振结果显示有两种不同的 Al 的占位，证实了耦合取代机制；然而随着压力提高，一些状态方程的结果与空位取代一致[20]。Al^{3+}的取代使得单胞体积和畸变程度同时增大，可能是由于 A 和 B 两个位置的取代导致堆积不充分，产生了(Mg, Al) (Si, Al)O_3成分。这一结果与 Kojitani 等人的结构精修结果一致，他们比较了两种取代机制合成的钙钛矿，结果表明，化学计量的含铝的$MgSiO_3$钙钛矿比非化学计量的$MgSiO_3$畸变程度更强。布里奇曼石最高可容纳 25 mol%的Al [21]。

其次，非化学计量替代产生的空穴可以被 H^+占据: $Si_B^{4+} = Al_B^{3+} + H^+$；或者被水与结构氧结合生成$OH^-$占据: $V_o^{\cdot\cdot} + O_o^{2-} + H_2O = 2OH_o^-$ [22] [23]。水以这样的方式进入布里奇曼石的晶格中，并存在于下地幔。

Fe^{3+}和Al^{3+}的耦合取代使得Fe^{3+}即使在下地幔还原环境中也能比较稳定[24]。布里奇曼石保持高价铁的能力使得下地幔富集Fe^{3+}和金属Fe，二者是一种平衡体系。实验观察到这种平衡，基于此，研究者们提出Fe^{2+}到Fe^{3+}和Fe0的歧化反应[25]。

布里奇曼石中Fe的自旋转变主要是由压力驱动的，其次是自旋翻转能减小[26]。Fe在镁钙钛矿中的行为是相当复杂的，这是由于Fe能适应多种结构占位(A位和B位)，价态(2^+, 3^+)和电子构型(高、低、中自旋) [27]。在下地幔压力下，Fe^{2+}在布里奇曼石中并没有经历自旋转变，但是其四极矩分裂作为压力的函数呈现出较大的变化，这与A位的晶格畸变增强一致[28] [29]。证据表明，含三价铁的布里奇曼石在B位的Fe^{3+}经历了一个从低自旋到高自旋的转变，而位于A位的Fe^{3+}保持高自旋构型[17]。伴随Fe^{3+}自旋转变，晶体体积会发生塌缩，自旋转变的压力区间大概是30~70 GPa。

随着下地幔压力的升高，布里奇曼石中Fe^{2+}的溶解度逐渐大。在无铝的样本中，最大溶解度(Fe/(Mg + Fe))的范围从25 GPa，1500℃条件下的0.16，增大到80 GPa条件下的至少0.74 [30]。最新的激光加热金刚石对顶砧实验报告了在95 GPa (~2100 km)高于2200 K的温压条件下，含Fe的布里奇曼石发生歧化反应，生成贫铁布里奇曼石相和一种未知的富铁硅酸盐相[31]。

4. 布里奇曼石的物理性质

布里奇曼石比铁方镁石的压缩性小。不像Fe^{3+}自旋转变导致的铁方镁石明显的体积和体积模量的降低，Fe^{3+}自旋转变对布里奇曼石的压缩性行为的影响较小。这可能为下地幔中部的地震波异常提供解释，而不需要考虑成分异常的影响[32] [33]。

布里奇曼石的热力学性质是理解下地幔动力学、热传导以及核幔热对流的关键。布里奇曼石的热传导系数和热容很大程度上决定了下地幔的绝热温度分布[34]，其本身的晶格热导率也由压力、温度和Fe的含量等因素决定。高温导致晶格热传导率减小，但是高压反而引起热导率增大，因此，在下地幔的范围内，热传导率可能保持不变或者变化不大[35] [36]。Tang等人的计算结果表明，下地幔压力条件下，不含铁的晶格热导率变化不大，室温条件下约为$10\ Wm^{-1}K^{-1}$，但是随着温度的升高降低[37]。Hsieh等人实验测得布里奇曼石的晶格热导率从下地幔顶部的~$10\ Wm^{-1}K^{-1}$上升到下地幔底部的~$20\ Wm^{-1}K^{-1}$，较大的晶格热导率的梯度可能是由于Fe的取代使得晶格畸变增强导致的[38] [39]。通过晶格热导率可以获得矿物的辐射热导率，进一步地得到地幔热导率约为$10\ Wm^{-1}K^{-1}$，这与实验结果大致相符[40]，但是仍然存在大概50%的误差。据此，可以得到核幔边界热通量：

$$\Phi(\varphi,\theta) = \Lambda(\varphi,\theta)\frac{T_{CMB} - T(\varphi,\theta,D)}{D}$$

T_{CMB}代表核幔边界的温度，T和Λ分别代表位置φ,θ的温度和热导率，D代表该位置距核幔边界的高程。结合布里奇曼石向后钙钛矿相变的温度，可以获得核幔边界的温度。在地球演化的早期，核幔边界的温度很高导致地核迅速冷却，引起内核的生长以及下地幔大面积的熔融。估计全球的通过核幔边界的热流超过7 TW (图3)，这也预示着地核的快速冷却[41]。而相变的克拉珀龙斜率是正值，大小取决于压力范围，热边界层厚度减小使得斜率更小，从而产生更大的核幔热流[42]。

科学家们使用布里渊散射的实验方法[11] [43]和理论计算([44], p.2) [45]得出布里奇曼石的声速。对比它和铁方镁石的剪切波和压缩波可以检测橄榄岩地幔的成分模型(图4)。Murakami等人[11]认为布里奇曼石在下地幔的岩石中占比超过90% [46]。布里奇曼石与球粒陨石具有相似的接近1.0的Mg/Si比，而地球上地幔的典型化学组成的Mg/Si摩尔比是~1.3 [4] [47]。上地幔的主要矿物是富Mg_2SiO_4的橄榄石，而球粒陨石的主要矿物是富集$MgSiO_3$的顽火辉石。这就是Si丢失悖论。考虑到下地幔的体积较大，更小的Mg/Si比能够调和固体地球的Mg/Si比与球粒陨石一致，科学家们预计有6~12 wt% Si存在于地核。
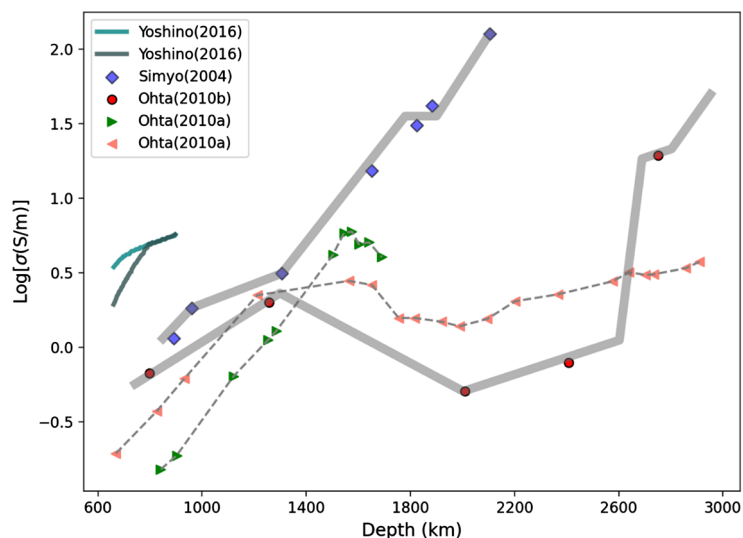
Figure 3. Electrical conductivity of bridgmanite under lower mantle conditions
图 3. 布里奇曼石在下地幔压力条件下的电导率

Figure 4. Heat transfer and water release in the deep mantle
图 4. 深部地幔的热传输和水的释放

电导率是地球内部的一个可观测的性质，可以通过地磁场的瞬时扰动获得。电导率对水和铁的成分非常敏感，通常，与水和 Fe 离子的浓度成正比，因此它能提供特定的地幔化学信息。由于电子与晶格的相互作用太强烈，价带理论对离子晶体不适用，离子晶体的电子通过热激发在不同位置间跃迁。对于布里奇曼石的导电机制，研究者们认为，在相对低温的条件下，Fe^{2+}-Fe^{3+}电子跃迁(小极化子)占主导，当温度升高，离子导电主导[48] (图 3)。由于布里奇曼石对温度更加敏感，在大压机中测量的天然布里奇曼石样本的电导率比过渡带矿物的电导率更高[48]。尽管 Fe^{3+}的自旋转变的影响存在争议，但是自旋转变之后配对电子减少，应该会导致布里奇曼石电导率减小，这与铁方镁石的性质一样[49] [50]。但是，Sinmyo等人发现在含 Al 的布里奇曼石中，Fe^{3+}的自旋转变对电导率几乎没有什么影响[50]。后钙钛矿具有层状结构，它的电导率高于布里奇曼石两个数量级，这能够提高地幔底部和液态外核的电磁耦合，有助于解释在十年时间尺度上的一天长度的变化([51], p.200) [52]。当布里奇曼石的中有 Al 掺杂，高温下的离子导电率随 Al 含量增加而上升。

地球大部分水以 H^+ 和 OH^- 的形式存在于造岩矿物中，从而储存在地壳、地幔甚至是地核中。钻石包体如橄榄石、石榴石、ice-VII 中含有少量的水，证明地幔中含水的，但是水的含量尚不确定[53] [54] [55]。

含水矿物中水的存在形式是 OH⁻，比如，云母、角闪石和绿泥石等，而这些含水相只在较低的温度条件下稳定存在。地幔中大部分的矿物相是名义上无水矿物(nominally anhydrous minerals)，如上文讨论的，水以 H 的形式微量存在于晶格缺陷或者与结构氧结合。

俯冲板块可以携带大量的水进入下地幔(图 4)，H 在名义上不含水矿物中扩散速率非常快，引起板块含水矿物脱水进入橄榄石、瓦兹利石和林伍德石中，因此过渡带是地球内部一个很大的水的储库。下地幔的含水矿物相有 phaseB (660~900 km)、phaseG (900~1200 km)等，但是这些相只存在于下地幔顶部温度较低的部分，且在下地幔占比有限[56]。下地幔大部分的水还是存在于名义上不含水矿物中，如布里奇曼石和铁方镁石。

地幔的含水量很难被测定，并存在很大争议。大压机实验报道了在含铝的布里奇曼石中含水量可达8000 ppm，表明下地幔是一个潜在的"储水池"[22] [57]。Fu 等人发现布里奇曼石单晶样品中含有~1020 (±70) pp 的水[58]。这些实验与地球化学估算吻合——水在洋岛玄武岩的地幔源区的蒸发浓度高达~1000 ppm，这里的水可能就来自下地幔[59]。相反地，早期实验和计算发现布里奇曼石中水的溶解度较低(大概 100 ppm 的浓度) [23]。Litasov 等人的研究还发现，H 的含量和 Al 的浓度有关，当 Al 的含量较低时，优先选择非化学计量，从而产生更多的空穴[23]。科学家们估计含铝的后钙钛矿能容纳的水是布里奇曼石的 5~10 倍[60]。晶格中的水影响矿物的熔融温度、粘性、电导率和地震波速等物理性质。地震波观察提供了水被运送至下地幔的直接证据：在下地幔顶部和核幔边界存在地震波低速区[61] [62] (图 5)。Schmandt 等人观测到在上地幔的顶部存在低速区，他们认为这是由于俯冲板块驱使林伍德石向下移动，发生部分熔融生成含水布里奇曼石，引起的地震波速骤减[63]。Townsend 等人认为，后钙钛矿脱掉的水会转移到在高温区域(部分熔融)转移到布里奇曼石中，观测结果发现该区域是一个大低速省(LLSVP) [62] [64]。

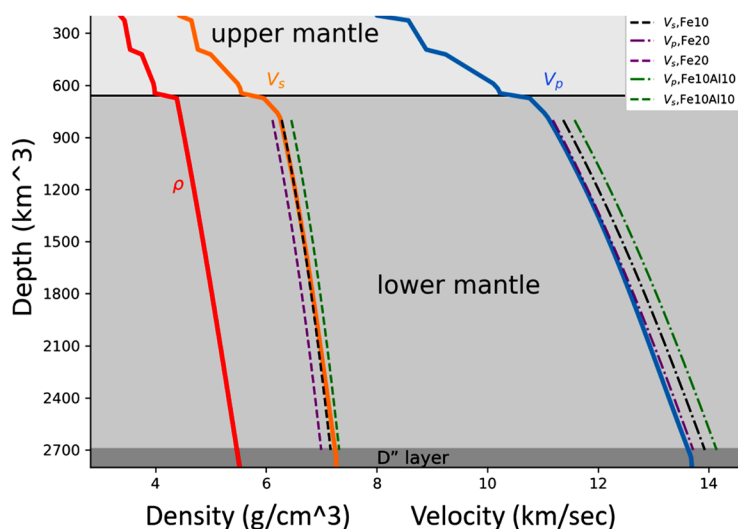**Figure 5.** Radial dependence of depth and P- and S-wave speeds in the PREM and bridgmanite
图 5. PREM 和布里奇曼石的 P 波和 S 波的波速

5. 布里奇曼石的 XRD 研究

由于布里奇曼石重要的地质学意义，研究人员对其晶体结构、电子状态、超精细结构分析等展开了大量的研究，研究手段包括单晶及粉晶的 X 射线研究(XRD) [65] [66] [67] [68]，同步辐射穆斯保尔谱(SMS) [33] [67]，X-射线反射谱(XAS) [67] [69]等。实验结果表明占据 B 位的 Fe³⁺会在大概 30~70 GPa 的压力范围经历一个从高自旋(HS)向低自旋(LS)的自旋转变(图 6)；而 Fe²⁺无论占据 A 位还是 B 位，都会在下地幔

的压力范围内保持高自旋[17] [27] [70] [71]。伴随 B 位 Fe^{3+} 的自旋转变，布里奇曼石晶体的体积会发生坍缩[67] [71]。另一方面，尽管位于 A 位的 Fe^{2+} 没有发生自旋转变，它所在的假十二面体结构会出现晶格畸变[29] [33] [67] [69]。随着压力的升高，随之改变的还有 Si-O 八面体的偏转角度[65]。有些研究将这一现象归因于位于 A 位的 Fe 的原子位置的变化而导致 A 位的压缩能力的改变[72] [73]，但是，目前尚没有实验室据证实这一理论解释。
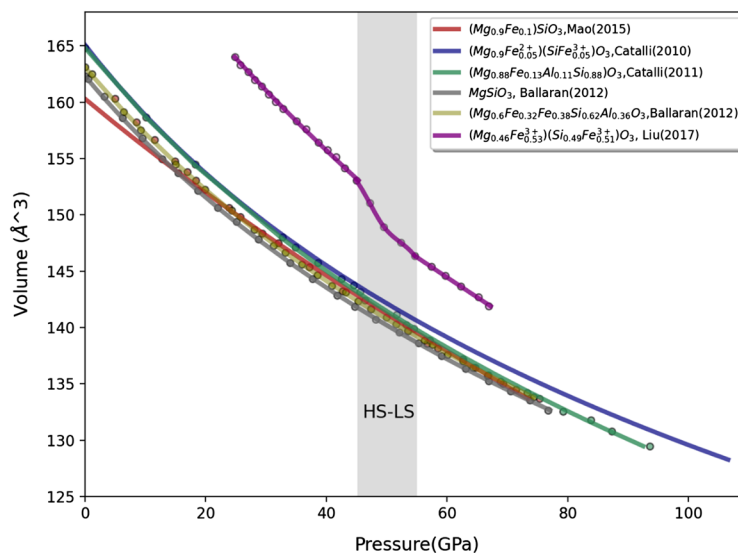

Figure 6. Volume evolution with increasing pressure for bridgmanite
图 6. 不同成分布里奇曼石的体积随压力的变化

针对钙钛矿型的镁硅酸盐($MgSiO_3$)的单晶 X 射线衍射研究已经开展了多年，但是这些实验都局限在较低的压力范围。Ross 等人[65]的 $MgSiO_3$ 的单晶衍射实验中，加压到 12.6 GPa，其结果表明 SiO_6 八面体发生旋转，尤其是在[bc]面，MgO_{12} 十二面体随着压力升高畸变程度增强。Sugahara 等人[74]的实验最高压力为 15 GPa，没有达到下地幔的压力条件。前人的结果表明晶体结构中的原子呈现出明显的热振动的各向异性，Mg、Si、O_2 原子中的最大振幅的原子的震动方向都朝向空间。除此之外，粉晶 X 射线衍射实验的能实现下地幔的压力条件，从而根据三阶 Birch-Murnaghan 状态方程计算等热体积模量。Mao 等人[33]将含铁(Fe-bearing)布里奇曼石以及含铁铝(Fe, Al-bearing)布里奇曼石加压到 125~130 GPa，并检验了其状态方程，他们认为铁的加入会使布里奇曼石的密度和体积模量增大，但同时会减弱体积声速；而铁和铝同时掺杂会使其对密度和体积模量的影响变小。

对布里奇曼石的物理性质的研究表明，其晶格结构中 Fe^{2+} 的畸变可能导致一些重要的变化。最近的高压下晶体的热传导研究发现，晶格畸变可能会引起强烈的晶格散射效应从而使得晶体的热导率下降一到两个数量级[38]。此外，有报道称晶格畸变可能对布里奇曼石在 45 GPa 压力下力常数的突降有影响[75]。因此，Fe^{2+}、Fe^{3+} 占据的 A 位的晶格畸变随着压力的变化需要被进一步探究。总之，使用同步辐射 X 射线散射技术测试布里奇曼石在高压条件下的晶格参数来限制其单晶结构具有十分重要的意义。

6. 总结

布里奇曼石是下地幔含量最多的矿物，它的晶体化学性质的改变可能引起物理性质的变化，进而影响下地幔的热力学、动力学等多种性质。Fe 和 Al 进入晶格使得它的结构进一步复杂。Fe^{2+} 和 Fe^{3+} 的占位情况不同，在地幔压力条件下的自旋转变情况也不同，Fe^{3+} 在 B 位的自旋转变的压力尚存在争议。Al 取

代 Si 和 Fe^{3+} 耦合取代机制会减弱自旋转变的发生可能性。自旋转变对下地幔物理性质的影响需要更多的实验和理论数据的支持。布里奇曼石的晶格热导率在整个下地幔变化不大。一般认为，布里奇曼石在低温下的导电机制是极化子跳跃，晶格中的 Fe、水和 Al 的含量对电导率影响很大。一些实验和理论计算说明布里奇曼晶格中有含量可观的水，但是，也有研究者认为它几乎不含水。对布里奇曼石的晶体学和物理性质的研究有非常重要的地质学意义。

参考文献

[1] Marquardt, H., Speziale S., Reichmann, H.J., Frost, D.J., Schilling, F.R. and Garnero, E.J. (2009) Elastic Shear Anisotropy of Ferropericlase in Earth's Lower Mantle. *Science*, **324**, 224-226. https://doi.org/10.1126/science.1169365

[2] Karki, B.B., Stixrude, L., Clark, S.J., Warren, M.C., Ackland, G.J. and Crain, J. (1997) Elastic Properties of Orthorhombic $MgSiO_3$ Perovskite at Lower Mantle Pressures. *American Mineralogist*, **82**, 635-638. https://doi.org/10.2138/am-1997-5-623

[3] Dobson, D.P. and Brodholt, J.P. (2000) The Electrical Conductivity of the Lower Mantle Phase Magnesiowüstite at High Temperatures and Pressures. *Journal of Geophysical Research*: *Solid Earth*, **105**, 531-538. https://doi.org/10.1029/1999JB900242

[4] Ringwood, A.E. (1975) Composition and Petrology of the Earth's Mantle. McGraw-Hill, New York. https://trove.nla.gov.au/version/44888034

[5] Kesson, S.E., Fitz Gerald, J.D. and Shelley, J.M. (1998) Mineralogy and Dynamics of a Pyrolite Lower Mantle. *Nature*, **393**, 252-255. https://doi.org/10.1038/30466

[6] Irifune, T., Kubo, N., Isshiki, M., *et al.* (1998) Phase Transformations in Serpentine and Transportation of Water into the Lower Mantle. *Geophysical Research Letters*, **25**, 203-206. https://doi.org/10.1029/97GL03572

[7] Ricolleau, A., Perrillat, J.-P, Fiquet G, Daniel, I., Matas, J., Addad, A., *et al.* (2010) Phase Relations and Equation of State of a Natural MORB: Implications for the Density Profile of Subducted Oceanic Crust in the Earth's Lower Mantle. *Journal of Geophysical Research*, **115**, Article ID: B08202. https://doi.org/10.1029/2009JB006709

[8] Tschauner, O., Ma, C., Beckett, J.R., Prescher, C., Prakapenka, V.B. and Rossman, G.R. (2014) Mineralogy. Discovery of Bridgmanite, the Most Abundant Mineral in Earth, in a Shocked Meteorite. *Science*, **346**, 1100-1102. https://doi.org/10.1126/science.1259369

[9] Boehler, R. (2000) High-Pressure Experiments and the Phase Diagram of Lower Mantle and Core Materials. *Reviews of Geophysics*, **38**, 221-245. https://doi.org/10.1029/1998RG000053

[10] Nishiyama, N. and Yagi, T. (2003) Phase Relation and Mineral Chemistry in Pyrolite to 2200°C under the Lower Mantle Pressures and Implications for Dynamics of Mantle Plumes: Phase Relation and Chemistry in Pyrolite. *Journal of Geophysical Research*: *Solid Earth*, **108**, Article No. 2255. http://doi.wiley.com/10.1029/2002JB002216 https://doi.org/10.1029/2002JB002216

[11] Murakami, M., Ohishi, Y., Hirao, N. and Hirose, K. (2012) A Perovskitic Lower Mantle Inferred from High-Pressure, High-Temperature Sound Velocity Data. *Nature*, **485**, 90-94. https://doi.org/10.1038/nature11004

[12] Hirose, K., Sinmyo, R. and Hernlund, J. (2017) Perovskite in Earth's Deep Interior. *Science*, **358**, 734-738. https://doi.org/10.1126/science.aam8561

[13] Wang, D. and Angel, R.J. (2011) Octahedral Tilts, Symmetry-Adapted Displacive Modes and Polyhedral Volume Ratios in Perovskite Structures. *Acta Crystallographica Section B Structural Science*, **67**, 302-314. https://doi.org/10.1107/S0108768111018313

[14] Fiquet, G., Guyot, F., Kunz, M., Matas, J., Andrault, D. and Hanfland, M. (2002) Structural Refinements of Magnesite at Very High Pressure. *American Mineralogist*, **87**, 1261-1265. https://doi.org/10.2138/am-2002-8-927

[15] Ito, E., Kubo, A., Katsura, T., Akaogi, M. and Fujita, T. (1998) High-Pressure Transformation of Pyrope $(Mg_3Al_2Si_3O_{12})$ in a Sintered Diamond Cubic Anvil Assembly. *Geophysical Research Letters*, **25**, 821-824. https://doi.org/10.1029/98GL00519

[16] Kudoh, Y., Prewitt, C.T., Finger, L.W., Darovskikh, A. and Ito, E. (1990) Effect of Iron on the Crystal Structure of $(Mg,Fe)SiO_3$ Perovskite. *Geophysical Research Letters*, **17**, 1481-1484. https://doi.org/10.1029/GL017i010p01481

[17] Catalli, K., Shim, S.-H., Prakapenka, V.B., Zhao, J.Y., Sturhahn, W., Chow, P., *et al.* (2010) Spin State of Ferric Iron in $MgSiO_3$ Perovskite and Its Effect on Elastic Properties. *Earth and Planetary Science Letters*, **289**, 68-75. https://doi.org/10.1016/j.epsl.2009.10.029

[18] Yamamoto, T., Yuen, D.A. and Ebisuzaki, T. (2003) Substitution Mechanism of Al Ions in $MgSiO_3$ Perovskite under

High Pressure Conditions from First-Principles Calculations. *Earth and Planetary Science Letters*, **206**, 617-625. https://doi.org/10.1016/S0012-821X(02)01099-3

[19] Akber-Knutson, S. and Bukowinski, M.S.T. (2004) The Energetics of Aluminum Solubility into $MgSiO_3$ Perovskite at Lower Mantle Conditions. *Earth and Planetary Science Letters*, **220**, 317-330. https://doi.org/10.1016/S0012-821X(04)00065-2

[20] Andrault, D. (2007) Properties of Lower Mantle Al-(Mg,Fe) SiO_3 Perovskite. *Special Papers—Geological Society of America*, **421**, 15-36. https://doi.org/10.1130/2007.2421(02)

[21] Kojitani, H., Katsura, T. and Akaogi, M. (2007) Aluminum Substitution Mechanisms in Perovskite-Type MgSiO3: An Investigation by Rietveld Analysis. *Physics and Chemistry of Minerals*, **34**, 257-267. https://doi.org/10.1007/s00269-007-0144-z

[22] Hernández, E.R., Alfè, D. and Brodholt, J. (2013) The Incorporation of Water into Lower-Mantle Perovskites: A First-Principles Study. *Earth and Planetary Science Letters*, **364**, 37-43. https://doi.org/10.1016/j.epsl.2013.01.005

[23] Litasov, K., Ohtani, E., Langenhorst, F., Yurimoto, H., Kubo, T. and Kondo, T. (2003) Water Solubility in Mg-Perovskites and Water Storage Capacity in the Lower Mantle. *Earth and Planetary Science Letters*, **211**, 189-203. https://doi.org/10.1016/S0012-821X(03)00200-0

[24] Frost, D.J. and Mccammon, C.A. (2008) The Redox State of Earth's Mantle. Annual Review of Earth and Planetary Sciences, **36**, 389-420. https://doi.org/10.1146/annurev.earth.36.031207.124322

[25] Frost, D.J., Liebske, C., Langenhorst, F., McCammon, C.A., Trønnes, R.G. and Rubie, D.C. (2004) Experimental Evidence for the Existence of Iron-Rich Metal in the Earth's Lower Mantle. *Nature*, **428**, 409-412. https://doi.org/10.1038/nature02413

[26] Bengtson, A., Persson, K. and Morgan, D. (2008) *Ab Initio* Study of the Composition Dependence of the Pressure-Induced Spin Crossover in Perovskite $(Mg_{1-x},Fe_x)SiO_3$. *Earth and Planetary Science Letters*, **265**, 535-545. https://doi.org/10.1016/j.epsl.2007.10.049

[27] Lin, J.-F., Speziale, S., Mao, Z. and Marquardt, H. (2013) Effects of the Electronic Spin Transitions of Iron in Lower Mantle Minerals: Implications for Deep Mantle Geophysics and Geochemistry: Spin Transition in Lower Mantle. *Reviews of Geophysics*, **51**, 244-275. https://doi.org/10.1002/rog.20010

[28] Jackson, J.M., Sturhahn, W., Shen, G., Zhao, J., Hu, M.Y., Errandonea, D., *et al*. (2005) A Synchrotron Mössbauer Spectroscopy Study of $(Mg,Fe)SiO_3$ Perovskite up to 120 GPa. *American Mineralogist*, **90**, 199-205. https://doi.org/10.2138/am.2005.1633

[29] Hsu, H., Umemoto, K., Blaha, P. and Wentzcovitch, R.M. (2010) Spin States and Hyperfine Interactions of Iron in $(Mg,Fe)SiO_3$ Perovskite under Pressure. *Earth and Planetary Science Letters*, **294**, 19-26. https://doi.org/10.1016/j.epsl.2010.02.031

[30] Dorfman, S.M., Meng, Y., Prakapenka, V.B. and Duffy, T.S. (2013) Effects of Fe-Enrichment on the Equation of State and Stability of $(Mg,Fe)SiO_3$ Perovskite. *Earth and Planetary Science Letters*, **361**, 249-257. https://doi.org/10.1016/j.epsl.2012.10.033

[31] Zhang, L., Meng, Y., Dera, P., Yang, W., Mao, W.L. and Mao, H.-K. (2013) Single-Crystal Structure Determination of $(Mg,Fe)SiO_3$ Postperovskite. *Proceedings of the National Academy of Sciences of the United States of America*, **110**, 6292-6295. https://doi.org/10.1073/pnas.1304402110

[32] Ballaran, T.B., Kurnosov, A., Glazyrin, K., Frost, D.J., Merlini, M., Hanfland, M., *et al*. (2012) Effect of Chemistry on the Compressibility of Silicate Perovskite in the Lower Mantle. *Earth and Planetary Science Letters*, **333**-**334**, 181-190. https://doi.org/10.1016/j.epsl.2012.03.029

[33] Mao, Z., Wang, F., Lin, J.-F., Fu, S., Yang, J., Wu, X., *et al*. (2017) Equation of State and Hyperfine Parameters of High-Spin Bridgmanite in the Earth's Lower Mantle by Synchrotron X-Ray Diffraction and Mössbauer Spectroscopy. *American Mineralogist*, **102**, 357-368. https://doi.org/10.2138/am-2017-5770

[34] Katsura, T., Yoneda, A., Yamazaki, D., Yoshino, T. and Ito, E. (2010) Adiabatic Temperature Profile in the Mantle. *Physics of the Earth and Planetary Interiors*, **183**, 212-218. https://doi.org/10.1016/j.pepi.2010.07.001

[35] Manthilake, G.M., de Koker, N., Frost, D.J. and McCammon, C.A. (2011) Lattice Thermal Conductivity of Lower Mantle Minerals and Heat Flux from Earth's Core. *Proceedings of the National Academy of Sciences of the United States of America*, **108**, 17901-17904. https://doi.org/10.1073/pnas.1110594108

[36] Ohta, K., Cohen, R.E., Hirose, K., Haule, K., Shimizu, K. and Ohishi, Y. (2012) Experimental and Theoretical Evidence for Pressure-Induced Metallization in FeO with Rocksalt-Type Structure. *Physical Review Letters*, **108**, Article ID: 026403. https://link.aps.org/doi/10.1103/PhysRevLett.108.026403 https://doi.org/10.1103/PhysRevLett.108.026403

[37] Tang, X., Ntam, M.C., Dong, J., Rainey, E.S.G. and Kavner, A. (2014) The Thermal Conductivity of Earth's Lower Mantle: Thermal Conductivity of Earth's Mantle. *Geophysical Research Letters*, **41**, 2746-2752.

https://doi.org/10.1002/2014GL059385

[38] Hsieh, W.-P., Deschamps, F., Okuchi, T. and Lin, J.-F. (2018) Effects of Iron on the Lattice Thermal Conductivity of Earth's Deep Mantle and Implications for Mantle Dynamics. *Proceedings of the National Academy of Sciences of the United States of America*, **115**, 4099-4104. https://doi.org/10.1073/pnas.1718557115

[39] Hsieh, W.-P., Deschamps, F., Okuchi, T. and Lin, J.-F. (2017) Reduced Lattice Thermal Conductivity of Fe-Bearing Bridgmanite in Earth's Deep Mantle: Reduced Conductivity of Fe-Bridgmanite. *Journal of Geophysical Research: Solid Earth*, **122**, 4900-4917. https://doi.org/10.1002/2017JB014339

[40] Goncharov, A.F., Beck, P., Struzhkin, V.V., Haugen, B.D. and Jacobsen, S.D. (2009) Thermal Conductivity of Lower-Mantle Minerals. *Physics of the Earth and Planetary Interiors*, **174**, 24-32. https://doi.org/10.1016/j.pepi.2008.07.033

[41] Tateno, S., Hirose, K., Sata, N. and Ohishi, Y. (2009) Determination of Post-Perovskite Phase Transition Boundary up to 4400 K and Implications for Thermal Structure in D" Layer. *Earth and Planetary Science Letters*, **277**, 130-136. https://doi.org/10.1016/j.epsl.2008.10.004

[42] Ye, Y., Prakapenka, V., Meng, Y. Shim, S.-H. (2017) Intercomparison of the Gold, Platinum, and MgO Pressure Scales up to 140 GPa and 2500 K. *Journal of Geophysical Research*: *Solid Earth*, **122**, 3450-3464. https://doi.org/10.1002/2016JB013811

[43] Kurnosov, A., Marquardt, H., Frost, D.J., Boffa Ballaran, T. and Ziberna, L. (2017) Evidence for a Fe^{3+}-Rich Pyrolitic Lower Mantle from (Al,Fe)-Bearing Bridgmanite Elasticity Data. *Nature*, **543**, 543-546. https://doi.org/10.1038/nature21390

[44] Wang, Q. (n.d.) A Computational Study of Calcium Carbonate. PhD Thesis, University College London, London, 215

[45] Wentzcovitch, R.M., Karki, B.B., Karato, S. and Da Silva, C.R.S. (1998) High Pressure Elastic Anisotropy of $MgSiO_3$ Perovskite and Geophysical Implications. *Earth and Planetary Science Letters*, **164**, 371-378. https://doi.org/10.1016/S0012-821X(98)00230-1

[46] Cottaar, S., Heister, T., Rose, I. and Unterborn, C. (2014) BurnMan: A Lower Mantle Mineral Physics Toolkit. *Geochemistry*, *Geophysics*, *Geosystems*, **15**, 1164-1179. https://doi.org/10.1002/2013GC005122

[47] Dziewonski, A.M. and Anderson, D.L. (1981) Preliminary Reference Earth Model. *Physics of the Earth and Planetary Interiors*, **25**, 297-356. https://doi.org/10.1016/0031-9201(81)90046-7

[48] Yoshino, T., Kamada, S., Zhao, C., Ohtani, E. and Hirao, N. (2016) Electrical Conductivity Model of Al-Bearing Bridgmanite with Implications for the Electrical Structure of the Earth's Lower Mantle. *Earth and Planetary Science Letters*, **434**, 208-219. https://doi.org/10.1016/j.epsl.2015.11.032

[49] Ohta, K., Hirose, K., Shimizu, K., Sata, N. and Ohishi, Y. (2010) The Electrical Resistance Measurements of $(Mg,Fe)SiO_3$ Perovskite at High Pressures and Implications for Electronic Spin Transition of Iron. *Physics of the Earth and Planetary Interiors*, **180**, 154-158. https://doi.org/10.1016/j.pepi.2009.11.002

[50] Sinmyo, R., Pesce, G., Greenberg, E., McCammon, C. and Dubrovinsky, L. (2014) Lower Mantle Electrical Conductivity Based on Measurements of Al, Fe-Bearing Perovskite under Lower Mantle Conditions. *Earth and Planetary Science Letters*, **393**, 165-172. https://doi.org/10.1016/j.epsl.2014.02.049

[51] Ohta, K., Onoda, S., Hirose, K., Sinmyo, R., Shimizu, K., Sata, N., *et al.* (2008) The Electrical Conductivity of Post-Perovskite in Earth's D" Layer. *Science*, **320**, 89-91. https://doi.org/10.1126/science.1155148

[52] Holme, R. (1998) Electromagnetic Core—Mantle Coupling—I. Explaining Decadal Changes in the Length of Day. *Geophysical Journal International*, **132**, 167-180. https://doi.org/10.1046/j.1365-246x.1998.00424.x

[53] Tschauner, O., Huang, S., Greenberg, E., Prakapenka, V.B., Ma, C., Rossman, G.R., *et al.* (2018) Ice-VII Inclusions in Diamonds: Evidence for Aqueous Fluid in Earth's Deep Mantle. *Science*, **359**, 1136-1139. https://doi.org/10.1126/science.aao3030

[54] Novella, D., Bolfan-Casanova, N., Nestola, F. and Harris, J.W. (2015) H_2O in Olivine and Garnet Inclusions Still Trapped in Diamonds from the Siberian Craton: Implications for the Water Content of Cratonic Lithosphere Peridotites. *Lithos*, **230**, 180-183. https://doi.org/10.1016/j.lithos.2015.05.013

[55] Nestola, F. and Smyth, J.R. (2016) Diamonds and Water in the Deep Earth: A New Scenario. *International Geology Review*, **58**, 263-276. https://doi.org/10.1080/00206814.2015.1056758

[56] Ohtani, E., Toma, M., Litasov, K., Kubo, T. and Suzuki, A. (2001) Stability of Dense Hydrous Magnesium Silicate Phases and Water Storage Capacity in the Transition Zone and Lower Mantle. *Physics of the Earth and Planetary Interiors*, **124**, 105-117. https://doi.org/10.1016/S0031-9201(01)00192-3

[57] Kakizawa, S., Inoue, T., Suenami, H. and Kikegawa, T. (2015) Decarbonation and Melting in $MgCO_3$-SiO_2 System at High Temperature and High Pressure. *Journal of Mineralogical and Petrological Sciences*, **110**, 179-188. https://doi.org/10.2465/jmps.150124

[58] Fu, S., Yang, J., Karato, S., Vasiliev, A., Presniakov, M.Y., Gavriliuk, A.G., *et al*. (2019) Water Concentration in Single-Crystal (Al,Fe)-Bearing Bridgmanite Grown From the Hydrous Melt: Implications for Dehydration Melting at the Topmost Lower Mantle. *Geophysical Research Letters*, **46**, 10346-10357. https://doi.org/10.1029/2019GL084630

[59] Dixon, J.E. and Clague, D.A. (2001) Volatiles in Basaltic Glasses from Loihi Seamount, Hawaii: Evidence for a Relatively Dry Plume Component. *Journal of Petrology*, **42**, 627-654. https://doi.org/10.1093/petrology/42.3.627

[60] Bolfan-Casanova, N., Keppler, H. and Rubie, D.C. (2000) Water Partitioning between Nominally Anhydrous Minerals in the MgO-SiO_2-H_2O System up to 24 GPa: Implications for the Distribution of Water in the Earth's Mantle. *Earth and Planetary Science Letters*, **182**, 209-221. https://doi.org/10.1016/S0012-821X(00)00244-2

[61] Tauzin, B., Debayle, E. and Wittlinger, G. (2010) Seismic Evidence for a Global Low-Velocity Layer within the Earth's Upper Mantle. *Nature Geoscience*, **3**, 718-721. https://doi.org/10.1038/ngeo969

[62] Yuan, K. and Romanowicz, B. (2017) Seismic Evidence for Partial Melting at the Root of Major Hot Spot Plumes. *Science*, **357**, 393-397. https://doi.org/10.1126/science.aan0760

[63] Brandon, S., Steven, J., Thorsten, B., Liu, Z. and Dueker, K.G. (2014) Dehydration Melting at the Top of the Lower Mantle. *Science*, **344**, 1265-1268. https://doi.org/10.1126/science.1253358

[64] Townsend, J.P., Tsuchiya, J., Bina, C.R. and Jacobsen, S.D. (2016) Water Partitioning between Bridgmanite and Postperovskite in the Lowermost Mantle. *Earth and Planetary Science Letters*, **454**, 20-27. https://doi.org/10.1016/j.epsl.2016.08.009

[65] Ross, N.L. and Hazen, R.M. (1990) High Pressure Crystal Chemistry of $MgSiO_3$ Perovskite. *Physics and Chemistry of Minerals*, **17**, 228-237. https://doi.org/10.1007/BF00201454

[66] Fiquet, G., Andrault, D., Dewaele, A., Charpin, T., Kunz, M. and Haüsermann, D. (1998) *P-V-T* Equation of State of $MgSiO_3$ Perovskite. *Physics of the Earth and Planetary Interiors*, **105**, 21-32. https://doi.org/10.1016/S0031-9201(97)00077-0

[67] Mao, Z., Lin, J.-F., Yang, J., Inoue, T. and Prakapenka, V.B. (2015) Effects of the Fe^{3+} Spin Transition on the Equation of State of Bridgmanite: Fe^{3+} Spin Transition in Bridgmanite. *Geophysical Research Letters*, **42**, 4335-4342. https://doi.org/10.1002/2015GL064400

[68] Wolf, A.S., Jackson, J.M., Dera, P. and Prakapenka, V.B. (2015) The Thermal Equation of State of (Mg, Fe)SiO_3 Bridgmanite (Perovskite) and Implications for Lower Mantle Structures: Fe Bridgmanite EOS and Mantle Structures. *Journal of Geophysical Research*: *Solid Earth*, **120**, 7460-7489. https://doi.org/10.1002/2015JB012108

[69] Lin, J.-F., Mao, Z., Yang, J., Liu, J., Xiao, Y., Chow, P., *et al*. (2016) High-Spin Fe^{2+} and Fe^{3+} in Single-Crystal Aluminous Bridgmanite in the Lower Mantle: Spin and Valence States of Bridgmanite. *Geophysical Research Letters*, **43**, 6952-6959. https://doi.org/10.1002/2016GL069836

[70] Catalli, K., Shim, S.-H., Dera, P., Prakapenka, V.B., Zhao, J., Sturhahn, W., *et al*. (2011) Effects of the Fe^{3+} Spin Transition on the Properties of Aluminous Perovskite—New Insights for Lower-Mantle Seismic Heterogeneities. *Earth and Planetary Science Letters*, **310**, 293-302. https://doi.org/10.1016/j.epsl.2011.08.018

[71] Liu, J., Dorfman, S.M., Zhu, F., Li, J., Wang, Y., Zhang, D., *et al*. (2018) Valence and Spin States of Iron Are Invisible in Earth's Lower Mantle. *Nature Communications*, **9**, Article No. 1284. https://doi.org/10.1038/s41467-018-03671-5 http://www.nature.com/articles/s41467-018-03671-5

[72] Hsu, H., Yu, Y.G., Wentzcovitch, R.M. (2012) Spin Crossover of Iron in Aluminous $MgSiO_3$ Perovskite and Post-Perovskite. *Earth and Planetary Science Letters*, **359**-**360**, 34-39. https://doi.org/10.1016/j.epsl.2012.09.029

[73] Hsu, H., Blaha, P., Cococcioni, M. and Wentzcovitch, R.M. (2011) Spin-State Crossover and Hyperfine Interactions of Ferric Iron in $MgSiO_3$ Perovskite. *Physical Review Letters*, **106**, Article ID: 118501. https://doi.org/10.1103/PhysRevLett.106.118501 https://link.aps.org/doi/10.1103/PhysRevLett.106.118501

[74] Sugahara, M., Yoshiasa, A., Komatsu, Y., Yamanaka, T., Bolfan-Casanova, N., Nakatsuka, A., *et al*. (2006) Reinvestigation of the $MgSiO_3$ Perovskite Structure at High Pressure. *American Mineralogist*, **91**, 533-536. https://doi.org/10.2138/am.2006.1980

[75] Yang, H., Lin, J.-F., Hu, M.Y., Roskosz, M., Bi, W., Zhao, J., *et al*. (2019) Iron Isotopic Fractionation in Mineral Phases from Earth's Lower Mantle: Did Terrestrial Magma Ocean Crystallization Fractionate Iron Isotopes? *Earth and Planetary Science Letters*, **506**, 113-122. https://doi.org/10.1016/j.epsl.2018.10.034